2010

Far-Field Optical Nanoscopy Based on Continuous Wave Laser Stimulated Emission Depletion

C. Kuang

Wei Zhao
zhao9@engr.sc.edu

Guiren Wang
University of South Carolina - Columbia, wanggu@cec.sc.edu

Publication Info

Published in *Review of Scientific Instruments*, Volume 81, 2010, pages 053709-1-053709-4.

AIP | Review of Scientific Instruments

Far-field optical nanoscopy based on continuous wave laser stimulated emission depletion

Cuifang Kuang, Wei Zhao, and Guiren Wang

Citation: Review of Scientific Instruments **81**, 053709 (2010); doi: 10.1063/1.3432001
View online: http://dx.doi.org/10.1063/1.3432001
View Table of Contents: http://scitation.aip.org/content/aip/journal/rsi/81/5?ver=pdfcov
Published by the AIP Publishing

Far-field optical nanoscopy based on continuous wave laser stimulated emission depletion

Cuifang Kuang,[1,2] Wei Zhao,[1] and Guiren Wang[1,a)]
[1]*Department of Mechanical Engineering and Biomedical Engineering Program, University of South Carolina, Columbia, South Carolina 29208, USA*
[2]*State Key Lab of Modern Optical Instrumentation, Zhejiang University, Hangzhou 310027, China*

(Received 17 March 2010; accepted 29 April 2010; published online 28 May 2010)

Stimulated emission depletion (STED) microscopy is one of the breakthrough technologies that belong to far-field optical microscopy and can achieve nanoscale spatial resolution. We demonstrate a far-field optical nanoscopy based on continuous wave lasers with different wavelengths, i.e., violet and green lasers for excitation and STED, respectively. Fluorescent dyes Coumarin 102 and Atto 390 are used for validating the depletion efficiency. Fluorescent nanoparticles are selected for characterizing the spatial resolution of the STED system. Linear scanning of the laser beams of the STED system along one line of a microscope slide, which is coated with the nanoparticles, indicates that a spatial resolution of about 70 nm has so far been achieved. A two-dimensional image of the particle pattern of the STED system is constructed and compared with scanning confocal microscope. The present work has further extended the application of the STED microscopy into the blue regime. © *2010 American Institute of Physics.* [doi:10.1063/1.3432001]

I. INTRODUCTION

Ultrahigh spatial resolution image of viable biological cell could provide insight for molecular biology, signal transduction and pathology, etc. Far-field fluorescence microscopy is one of most important tools for noninvasive imaging of interior of transparent objects. However, conventional optics for bioimaging suffers from Abbe's diffraction limit, which is about half the wavelength of the light used when nanoscale resolution is required.[1] This limit has been overcome with the advent of stimulated emission depletion (STED) microscopy, which is a lens-based fluorescence microscope with a resolution conceptually no longer limited by diffraction.[2] STED is part of the reversible saturable optical fluorescence transition concept[3] and was pioneered by Hell and Wichmann.[4] In this concept the fluorescent state is depleted by stimulated emission. STED fluorescence microscopy can theoretically achieve better than 5 nm spatial resolution,[5] even to the molecular scale. So far, a 5.8 nm spatial resolution, which demonstrates an all-physics-based far-field optical resolving power exceeding the wavelength of light by two orders of magnitude, has been achieved by Rittweger *et al.*[2] Up to now, most of the works reported use pulsed lasers for both excitation and STED.[2,3,6–18] Realization of a pulsed STED system requires a more complex optical setup and additional electric equipment. Using cw lasers can simplify the setup and significantly expand STED microscopy applications to perform high spatial resolution measurement. Another important benefit in cw STED microscopy is that one is working with low peak intensity since photo damage mechanisms scale with at least the square of the intensity of the irradiated light.[19] Recently, Willig *et al.*,[20] for the first time, demonstrated that the cw lasers can be used to STED microcopy as well. Then the same group (Han *et al.*[21]) further demonstrated that the cw lasers can image three-dimensional structure inside a diamond crystal. This cw laser STED system is for green fluorescent dyes. Another green laser depletion at 532 nm is reported in Rankin's work[22] but the laser is a pulsed light source. However, blue dyes are also widely used in bioimaging research. In addition to the aforementioned cw STED system, to our knowledge, there is no other report about cw STED. In this paper, we developed a cw laser STED nanoscopic system with different cw laser wavelengths. The system can be used for blue dyes and achieved about 70 nm spatial resolution for two-dimensional (2D) imaging.

II. EXPERIMENTAL SETUP

The schematic of the experiment setup used for the following measurements is shown in Fig. 1. The excitation beam is generated by a cw violet laser diode with a wavelength of 405 nm. The linear-polarized beam is aligned through a lens-pinhole-lens system, which includes lens (L_1), pinhole (PH_1), and lens (L_3) to expand the beam diameter. A dichroic mirror (DM_1) reflects the beam and the latter is reflected by a second dichroic mirror (DM_2). On the other hand, the STED beam is generated by a cw green laser diode with a wavelength of 532 nm. The linear-polarized STED beam is cleaned and expanded by another lens-pinhole-lens system which includes lens (L_2), pinhole (PH_2), and lens (L_4). The STED beam then passes through a half wave plate (WP_1) and phase plate (PP) (Vortex phase plate VPP-1, RPC photonic Inc., NY). The former makes the polarized direction of the STED beam to be the same as that of the excitation beam. The latter is used to generate a donut pattern of

a)Author to whom correspondence should be addressed. Tel.: +01 (803)-777-8013. FAX: +01 (803)-777-0106. Electronic mail: guirenwang@sc.edu.

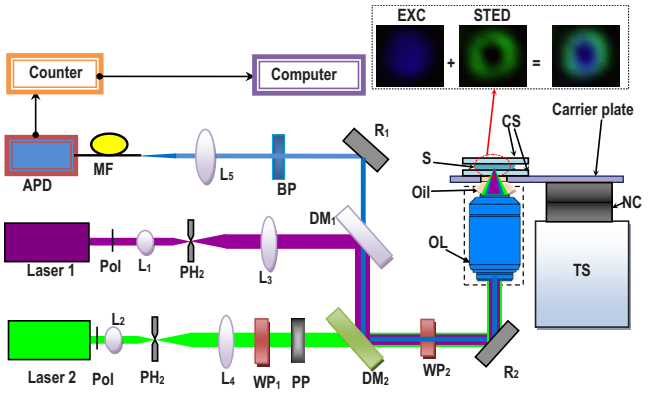

FIG. 1. (Color online) Schematic of the STED system setup. Laser 1: cw at 405 nm; laser 2: cw at 532 nm; L_1, L_2, L_3, L_4, and L_5: optical lenses; PH_1 and PH_2: pinholes; WP_1 and WP_2: wave plate (WP_1: half wave plate, WP_2: quarter wave plate); pol: light polarization direction; DM_1 and DM_2: dichroic mirrors (DM_1: R 405 nm, T 465 nm; DM_2: R 405 nm, T 532 nm); PP: phase plate (vortex mode); APD: avalanche photon detector; MF: multimode optical fiber (50 μm/125 μm); R_1 and R_2: reflector mirrors; BP: bandpass filter (440–490 nm); OL: objective lens (PlanApo,100X, NA=1.4 oil immersion); CS: cover slip (about 100 μm thickness); S: sample; NC: nanocube piezostage (three axis); TS: translation stage (three axis).

the STED beam. Downstream the DM_2, the two laser beams overlap and pass through a quarter wave plate (WP_2). The orientation of the fast axis of the quarter wave plate is set to 45° with reference to the polarized direction. The linear polarization state of the beam is changed to circular by this wave plate. The circular polarization beams are reflected by a reflector (R_2) and focused by an objective lens (OL, 100X, PlanApo, NA 1.4 oil immersions, Olympus, NY). In order to avoid what might mess up the circularity of the polarization, the metallic reflector (R_2) has been used here. The use of circular polarization for excitation, depletion, and detection yields a uniform effective resolution increase in the lateral directions of the focal plane of the objective lens. The focal doughnut of the STED laser is realized by the said phase plate. The sample is put between a cover slip and a microscope slide. Then, it is fixed on a nanocube (NC) piezoscanning stage (P-611.3FS, PI Inc., Germany) that can be scanned in all three spatial directions with a positioning resolution of 1 nm for fine tune. Another three-axis manual translation stage (TS) is used for rough adjustment. The fluorescent emitted by the sample is collected by the same objective lens and passes the two dichroic mirrors (DM_1 and DM_2). Then it is reflected by a reflector (R_1) and focused on a multimode optical fiber by the lens (L_5). The core diameter of the optical fiber is about 0.6 Airy disk to serve as the confocal pinhole. The pinhole can reject stray and ambient light noise. The other end of the optical fiber is connected to an ultralow noise single photon detection module (id100-MMF50, Becker & Hickl Inc., Germany). The bandpass filters are chosen between 440 and 490 nm, which are placed before the focusing lens (L_5). In order to minimize background light noise, three bandpass filters are used in series. The pulsed signal from the detector is counted by a pulse counter, then acquired by a PCI-GPIB interface, and saved to a computer.

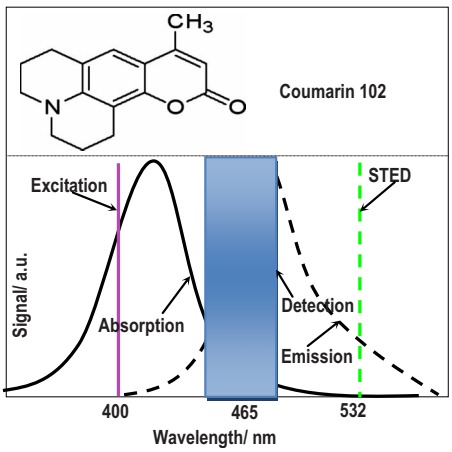

FIG. 2. (Color online) Optical property of the Coumarin 102 dye. The figure shows the structural formula of Coumarin 102, excitation and fluorescence spectrum, excitation and STED wavelength, and detection regions, respectively.

III. RESULTS AND DISCUSSION

A. Depletion efficiency validation

We will now test the depletion efficiency of this STED system in order to validate the stability and reliability of the system. The measurement is to test whether the fluorescence of a dye can be depleted by applying this STED laser or not. Since the intensity of the depletion beam can be three to four orders of magnitude higher than that of the excitation beam, the STED wavelength is commonly chosen on the red end of a dye's emission spectrum.[23] Here, the excitation and emission spectrums of the Coumarin 102 dye meet these requirements. Thus, it was chosen as a sample, which was used to test depletion efficiency of the system. The schematic of excitation and emission spectrum, the detection range, and the structural formula of the dye (Coumarin 102) are shown in Fig. 2.

To perform quantitative STED depletion measurement on a fluorescent dye, Coumarin 102 was prepared in a water solution. Meanwhile, the PP has to be removed from optical path. The experimental results of the STED depletion of fluorescence are shown in Fig. 3. The background with blocked excitation light and opened stimulating beam has been subtracted. In Fig. 3(a), A, C, and E segments are fluorescence signals with STED laser turned off, whereas B and D segments are with STED turned on at 450 mW downstream the objective. From Fig. 3(a), the photobleaching is not very serious under the relatively low intensity of the excitation (about 20 μW) since the signal intensity of the A, C, and E segments are almost same when the STED laser is turned off. The measurement has been done in a dye solution, which probably has a diffusion dye through the focus spot during the time of the laser turned off. Partially bleached molecules are probably already replaced by a new batch. Therefore, to prove accurately the low photobleaching, the high temporal resolution of laser shutter is needed or pulsed laser. Figure 3(b) is the experimental fluorescence suppression with increasing STED laser intensity. From Fig. 3(b), we can see that a strong reduction in the fluorescence signal can clearly be observed. With increasing power of the

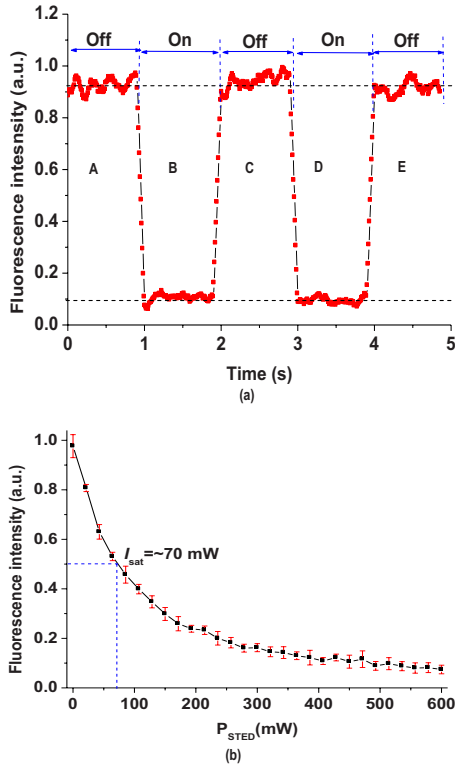

FIG. 3. (Color online) Fluorescence depletion of the Coumarin 102 dye. (a) Fluorescence intensity of Coumarin 102 solution with periodic switching on and off of the STED laser beam. (b) STED depletion efficiency of the cw mode laser for the dye.

cw STED laser beam, the fluorescence signal is gradually reduced. Eventually, the depletion efficiency achieved more than 90% with cw laser when the STED laser power is more than 400 mW. The maximal relative standard error of the depletion efficiency is 4.65%. The saturation intensity I_{sat} of the STED is about 70 mW, which can be defined as the intensity at which the probability of fluorescence emission is depleted by half.[24] The theoretical spatial resolution in lateral can be expressed as[25]

$$\Delta x \approx \frac{\lambda}{\pi n \sin\theta\sqrt{1 + I/I_{sat}}}, \quad (1)$$

where λ, n, and θ are beam wavelength, refractive index, and half aperture angle of the lens, respectively, and $n \sin\theta$ =NA denotes the numerical aperture (NA) of the objective lens. Thus, the effective resolution of a STED microscope is governed only by the NA and the square root of the saturation factor I/I_{sat}, where I is the intensity of the maximum of the donut. The spatial resolution can be estimated at about 40 nm using Eq. (1), when the parameters are set: NA=1.4, I =600 mW, λ=532 nm, and I_{sat}=70 mW. Here, the measuring STED efficiency curve in solution as shown in Fig. 3(b), throughout the focus, all values of STED intensities are present and the actual saturation intensity is rather at $1/e$ than 1/2. There, the prediction of the obtainable resolution is a probable approximation value. Above measurement results indicate the ability to perform high depletion efficiency with violet and green cw laser. In addition, in order to validate the other dye can be used in this system. The Atto 390 (Sigma-Aldrich Corp.) dye has been tested by the same experiments. The experimental results show that it has almost the same characteristic with Coumarin 102 dye.

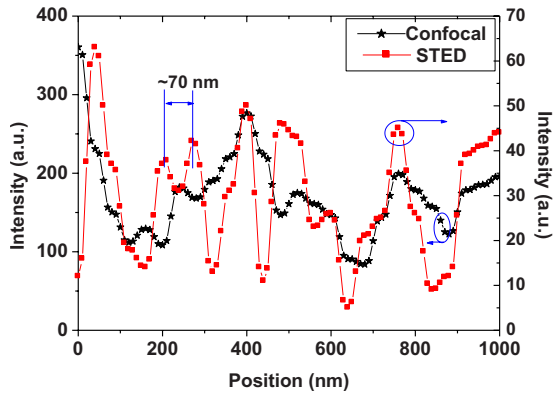

FIG. 4. (Color online) Comparison of spatial resolution between the cw STED system and confocal microscope. Fluorescence intensity profile of nanoparticles is measured to determine the smallest distance between two peaks that can be discriminated when the "focused" laser beam scans through various positions along a line.

B. High resolution measurements

Now that it is possible to deplete excited dye molecules with cw STED very efficiently, experiment on resolution evaluation was performed. This experiment with the above described setup was carried out in order to demonstrate the feasibility of cw green lasers for STED microscopy with diffraction-unlimited resolution. To determine the effective spatial resolution experimentally, a glass cover slip coated with fluorescence nanoparticles was scanned using both the STED and confocal techniques. The experimental results are shown in Fig. 4, when the power of the excitation and STED beams is about 25 μW and 650 mW, respectively. Here, the spatial resolution is defined as the smallest distance between two distinguished peaks.[26] These particles are distributed randomly on the slide. Hence, it is very difficult to find the smallest distance between two particles, which the STED system can distinguish. From Fig. 4, it is seen that the STED system has achieved at least a spatial resolution of 70 nm in the focal plane where nearby particles could be resolved and the full width at half maximum is much smaller, while the confocal technique cannot discriminate the two peaks from the particles. The above measurement results indicate the ability to perform high resolution (beyond Abbe's diffraction limit) measurement with violet and green cw laser. In comparison with the diffraction limit for confocal system (about 200 nm), this corresponds to a roughly threefold gain in the focal plane resolution and an approximately ninefold reduction in the lateral focal spot area. When the confocal experiment was done, the STED laser was just blocked. So, the sample does not need to be reinstalled. It will assure the position relation between the confocal and STED experiments in scanning direction.

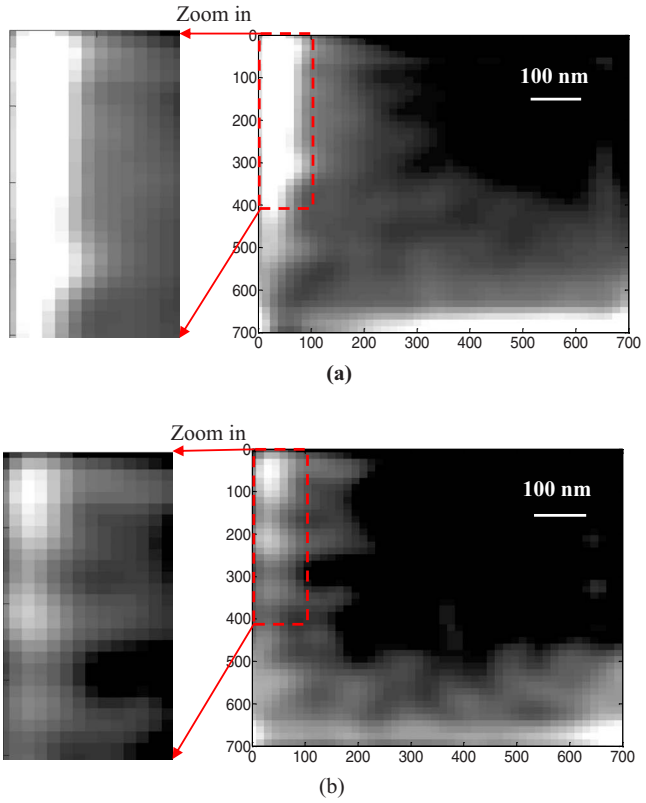

FIG. 5. (Color online) 2D Imaging of the nanoparticle distribution patterns: (a) confocal and (b) STED.

C. Nanoparticle image

In order to determine the imaging capability of the system, the pattern of fluorescent nanoparticles with diameter of about 100 nm randomly distributed on a slide was imaged. The maximum absorption and emission of the particles are at 398 and 460 nm, respectively. The average excitation and STED power at the sample were 25 μW and 600 mW, respectively. Several images using this 1.4 NA objective lens were recorded with a pixel spacing of 15×15 nm^2, both in the confocal and the STED modes, by turning the STED beam on and off for the relevant measurement. In the confocal image, the fine pattern of the particles could not be resolved in the zoom in image of Fig. 5(a), whereas in the STED image, the fine pattern can be resolved as shown in the zoom in image of Fig. 5(b). Figure 5 indicates that the presented STED system can significantly improve the spatial resolution for nanoscopic imaging. However, both images are blurry. On the left side, you can see an improvement but the rest of the image is dark. This is because the system scanning speed is slow (depending on the nanostage), resulting in fluorescence photobleaching. The imaging will be improved in the future via replacing a high response nanopiezostage or bleaching resistance fluorescent nanoparticles.

IV. SUMMARY

In summary, we have demonstrated a cw laser-based optical nanoscopic method. The developed STED system is a powerful tool for investigating fluorescence imaging. The blue dye is demonstrated for imaging and evaluation. Here, the spatial resolution is about 70 nm beyond the diffraction limit for 2D particles' image. The work could expand the application of cw STED. However, the further to the blue laser lines are, the more prominent bleaching will be, especially for the powerful STED beam. And one of the most important bleaching channels is due to triplet-state buildup[27] from where the sample bleaches easily. Triplet buildup happens easily in cw mode. Therefore, this is a key point for focusing on blue line laser STED imaging system in future.

ACKNOWLEDGMENTS

This work was financially supported by the by the NSF RII funding (Grant No. EPS-0447660).

[1] E. Abbe, Arch. Mikrosc. Anat. Entwicklungsmech. **9**, 413 (1873).
[2] E. Rittweger, K. Y. Han, S. E. Irvine, C. Eggeling, and S. W. Hell, Nat. Photonics **3**, 144 (2009).
[3] J. Keller, A. Schönle, and S. W. Hell, Opt. Express **15**, 3361 (2007).
[4] S. W. Hell and J. Wichmann, Opt. Lett. **19**, 780 (1994).
[5] S. W. Hell, Nat. Biotechnol. **21**, 1347 (2003).
[6] M. Dyba and S. W. Hell, Phys. Rev. Lett. **88**, 163901 (2002).
[7] V. Westphal, C. M. Blanca, M. Dyba, L. Kastrup, and S. W. Hell, Appl. Phys. Lett. **82**, 3125 (2003).
[8] M. Dyba, S. Jakobs, and S. W. Hell, Nat. Biotechnol. **21**, 1303 (2003).
[9] V. Westphal and S. W. Hell, Phys. Rev. Lett. **94**, 143903 (2005).
[10] K. I. Willig, S. O. Rizzoli, V. Westphal, R. Jahn, and S. W. Hell, Nature (London) **440**, 935 (2006).
[11] G. Donnert, J. Keller, R. Medda, M. A. Andrei, S. O. Rizzoli, R. Lührmann, R. Jahn, C. Eggeling, and S. W. Hell, Proc. Natl. Acad. Sci. U.S.A. **103**, 11440 (2006).
[12] G. Donnert, J. Keller, C. A. Wurm, S. O. Rizzoli, V. Westphal, A. Schönle, R. Jahn, S. Jakobs, C. Eggeling, and S. W. Hell, Biophys. J. **92**, L67 (2007).
[13] S. W. Hell, Science **316**, 1153 (2007).
[14] A. Schönle and S. W. Hell, Nat. Biotechnol. **25**, 1234 (2007).
[15] V. Westphal, M. A. Lauterbach, A. D. Nicola, and S. W. Hell, New J. Phys. **9**, 435 (2007).
[16] M. Bossi, J. Fölling, V. N. Belov, V. P. Boyarskiy, R. Medda, A. Egner, C. Eggeling, A. Schönle, and S. W. Hell, Nano Lett. **8**, 2463 (2008).
[17] B. Harke, C. K. Ullal, J. Keller, and S. W. Hell, Nano Lett. **8**, 1309 (2008).
[18] C. Eggeling, C. Ringemann, R. Medda, G. Schwarzmann, K. Sandhoff, S. Polyakova, V. N. Belov, B. Hein, C. von Middendorff, A. Schonle, and S. W. Hell, Nature (London) **457**, 1159 (2009).
[19] A. Hopt and E. Neher, Biophys. J. **80**, 2029 (2001).
[20] K. I. Willig, B. Harke, R. Medda, and S. W. Hell, Nat. Methods **4**, 915 (2007).
[21] K. Y. Han, K. I. Willig, E. Rittweger, F. Jelezko, C. Eggeling, and S. W. Hell, Nano Lett. **9**, 3323 (2009).
[22] B. R. Rankin, R. R. Kellner, and S. W. Hell, Opt. Lett. **33**, 2491 (2008).
[23] E. Rittweger, B. R. Rankin, V. Westphal, and S. W. Hell, Chem. Phys. Lett. **442**, 483 (2007).
[24] B. Harke, J. Keller, C. K. Ullal, V. Westphal, A. Schönle, and S. W. Hell, Opt. Express **16**, 4154 (2008).
[25] S. W. Hell, M. Dyba, and S. Jakobs, Curr. Opin. Neurobiol. **14**, 599 (2004).
[26] D. Wildanger, J. Bückers, V. Westphal, S. W. Hell, and L. Kastrup, Opt. Express **17**, 16100 (2009).
[27] G. Donnert, C. Eggeling, and S. W. Hell, Nat. Methods **4**, 81 (2007).